Taylor & Francis
Taylor & Francis Group

Corrosion Engineering, Science and Technology

The International Journal of Corrosion Processes and Corrosion Control

ISSN: (Print) (Online) Journal homepage: https://www.tandfonline.com/loi/ycst20

Formation of *Escherichia coli* biofilms on the titanium alloy Ti6Al4V: analysis of the interface and assessment of corrosion

Jonathan Calvillo, Mónica Galicia, Roxana Malpica, Elsa Ordoñez & Héctor Ferral Pérez

To cite this article: Jonathan Calvillo, Mónica Galicia, Roxana Malpica, Elsa Ordoñez & Héctor Ferral Pérez (2021): Formation of *Escherichia coli* biofilms on the titanium alloy Ti6Al4V: analysis of the interface and assessment of corrosion, Corrosion Engineering, Science and Technology, DOI: 10.1080/1478422X.2021.1901043

To link to this article: https://doi.org/10.1080/1478422X.2021.1901043

CORROSION ENGINEERING, SCIENCE AND TECHNOLOGY
https://doi.org/10.1080/1478422X.2021.1901043

The Institute of Materials, Minerals and Mining

Taylor & Francis
Taylor & Francis Group

RESEARCH ARTICLE

Formation of *Escherichia coli* biofilms on the titanium alloy Ti6Al4V: analysis of the interface and assessment of corrosion

Jonathan Calvillo [a], Mónica Galicia [a], Roxana Malpica [a], Elsa Ordoñez [b] and Héctor Ferral Pérez [a]

[a]Universidad Autónoma de Ciudad Juárez, Instituto de Ciencias Biomédicas, Ciudad Juárez, México; [b]Universidad Autónoma de Ciudad Juárez, Instituto de Ingeniería y Tecnología, Ciudad Juárez, México

ABSTRACT

Bacterial biofilm that formed when the Ti6Al4 V alloy was exposed to Escherichia coli, was monitored over 48 h by electrochemical impedance spectroscopy (EIS) and potentiodynamic polarization (PP) to estimate the rate of corrosion and the influence of the bacteria on this process. High-resolution scanning electron microscopy was used to examine bacterial growth, colonisation and the process of biofilm formation. Our results highlighted several critical points regarding the impact of E. coli and its use as a model for monitoring biofilm formation and the biocorrosion of this alloy. Impedance spectra revealed the formation of a compact passive film after 48-hour exposure to an aging culture of E. coli in chloride media. The formation of the biofilm influenced the resistance to corrosion. Biofilm impedance parameters that emerged over time corresponded directly to the properties of a typical exponential bacterial growth curve determined by ultraviolet-visible light spectroscopy.

ARTICLE HISTORY
Received 19 November 2020
Accepted 6 March 2021

KEYWORDS
Escherichia coli; biofilm; electrochemical impedance spectroscopy; potentiodynamic polarisation; titanium alloy

Introduction

The formulation of new titanium (Ti) alloys has led to the development of advanced materials with unique applications in the aerospace, automotive and chemical industries. These alloys have also facilitated important biomedical advances, including new surgical tools and dental implants [1–3]. The Ti alloy, Ti6Al4V, has been used extensively in orthopaedic and dental surgery due to its mechanical properties, high resistance to corrosion and biocompatibility with human tissues [4,5]. There is also increased emphasis focused on bacterial strains and species that might have an impact on Ti alloys, given the high likelihood that human implants will be subject to colonisation and that their surfaces will become sites of biofilm formation [6–10]. The nature and degree of microbiological colonisation and biofilm formation are unique physicochemical properties that are characteristic of each alloy. The impact of these processes cannot be interpreted as one would a simple inorganic process, even in cases when corrosion is the only process involved [11,12]. When considering the impact of microorganism exposure on a given metal or alloy, the following issues need to be considered:

(1) the nature of the microbes colonising the metal surface.
(2) the extent of consolidation of the biofilm that develops due to microbial colonisation; and
(3) the nature of the resulting biofilm.

Microbes that are most likely to initiate corrosion are those that promote biofilm formation and excrete corrosive metabolites and extracellular polymeric substances (EPSs), which are the main structural components of biofilms [13,14].

From the electrochemical point of view, a highly consolidated biofilm established on the surface of an alloy may serve as a barrier that impedes the active corrosion process. For example, Galicia et al. [15] explored the impact of marine biofilm formation on coated carbon steel immersed in sea water. Using open circuit potential (OCP) monitoring and electrochemical impedance spectroscopy (EIS), these researchers found that the biofilm that formed on the coated steel protected it from corrosion at the earliest time points in their experiments. More recently, Calvillo and Galicia [16] presented impedance diagrams that revealed adherence and attachment of *Shewanella sp*. and biofilm formation on coated carbon steel beginning at the first day of immersion; this was followed by biofilm detachment several days later. Collectively, these results revealed enhanced resistance to corrosion and suggested that marine biofilms promoted a barrier against the active dissolution of carbon-coated steel. Similar electrochemical behaviour was described by Castaneda and Galicia [17] in their description of an extra biolayer that formed on a coating surface that originally resulted from the actions of a sulfate-reducing bacterial consortium. In this case, the researchers found that bacterial secretion of EPSs resulted in the formation of a more homogeneous biolayer that served as a barrier against corrosion.

Ti and its alloys have emerged as excellent materials for use in biomedical implants due to their critical mechanical and anti-corrosion properties. Several studies that focused on the electrochemical behaviour of pure Ti have revealed several of these important biomedical properties [18–20]. However, and despite their remarkable utility particularly for biomedical applications, Ti and its alloys, including Ti6Al4V, remain susceptible to significant biofilm formation. This finding is of significant

CONTACT Mónica Galicia monica.galicia@uacj.mx Universidad Autónoma de Ciudad Juárez, Instituto de Ciencias Biomédicas, Av. Plutarco Elías Calles No. 1210, Ciudad Juárez, México

concern given the potential for human toxicity. Dhaliwal et al. [21] reviewed the impact of aerobic and anaerobic bacterial biofilms using scanning electron microscopy (SEM) and confocal laser scanning microscopy. Other studies focused on bacterial toxicity and the control of biofilm formation on Ti alloys used in biomedical applications [22–24].

Escherichia coli is a well-characterised, ubiquitous Gram-negative bacteria with standardised methods available for experimental measurement and manipulation. Cwalina et al. [25] reported that corrosion of low carbon steel in the presence of aerobic *E. coli* could be attributed to bacterial secretion of metabolic organic acids. Bacterial growth typically results in significant reductions in the pH of electrolytic media due to the production and release of organic acids during sugar metabolism. As acidification serves to initiate metal dissolution, reductions in pH generated by bacterial growth alone can promote the corrosion process. Moreover, *E. coli* can adhere to metal surfaces, thereby promoting the formation of biofilms. Ma et al. [26] reported that *E. coli* can grow on the surface of stainless steel at 22°C and can form biofilms on this material for up to 24 h. Others have reported that *E. coli* can grow on Ti surfaces [27]. *E. coli* biofilms on Ti that form within 48 h of initial exposure have been evaluated by SEM [28].

This study focuses on the impact of bacterial biofilms on the corrosion of a Ti alloy. *E. coli* exhibits strong growth in a medium containing Ti ions, a finding that is consistent with the susceptibility of this metal to biofilm formation [26]. Moreover, it has been shown *in vitro* that corrosion of Grade 2 Ti was amplified in the presence of saliva containing *E. coli* lipopolysaccharide (LPS) and at low pH [27]. The zones undergoing reduced aeration can serve as an anode and will undergo crevice corrosion, thereby releasing metal ions into the environment. The combination of bacterial end products, released metal ions and chloride ions present in electrolyte media will serve to establish an environment that promotes corrosion of the Ti alloy surface [28].

Ti alloys, notably Ti6Al4V, are highly susceptible to biofilm formation as their biocompatibility with human tissues favours the attachment of multiple microorganisms [29–31]. Impedance analysis facilitated the monitoring of the growth and activity of bacteria frequently found in Ti6Al4V-associated biofilms as well as the impact of bacterial-derived biomolecules (i.e. mainly carbohydrates, ions and proteins) via their interactions with this alloy [32]. As previously described by Cortez et al. [33], changes in electrical resistance and capacitance provide an overview of redox processes and associated interactions with the components of the media including bacteria [33].

Given the importance of these initial findings, we need to have an in-depth understanding of the electrochemical properties of *E. coli*-based biofilms that can form on Ti alloys. In this study, we present a study of the nature and extent of Ti6Al4V corrosion in the presence of *E. coli* in a chloride-containing environment using both EIS and potentiodynamic polarisation (PP). Our findings also reveal a direct correlation between the activity of *E. coli* and its morphological impact on the surface of the Ti6Al4V alloy.

Table 1. Content of LB broth.

Components	Amount/g L^{-1}
NaCl	10
Yeast extract	5
Tryptone	10

Materials and methods

Inoculation of microorganisms and bacteria manipulation

Escherichia coli MC4100 was stored at −80°C in Luria Bertani (LB) broth (Sigma Aldrich) supplemented with glycerol. One day before performing the assays, *E. coli* was sub-cultured in LB broth (pH adjusted to 7.2) and incubated at 37°C for 12 h. On the day that the assay was performed, the overnight culture was used to inoculate LB broth in the electrochemical cell (see composition in Table 1). Electrochemical measurements were collected for 48 h at 23°C.

Preparation of the electrode

The electrodes consisted of blocks of Ti6Al4V alloy (10 × 11 × 3 mm) in a rectangular case mounted with an epoxy resin that exposed a rectangular surface of 1.10 cm^2. The exposed surface was polished to a mirror finish with a diamond powder solution and a microfiber cloth. The reference electrode was a saturated calomel electrode (SCE). A platinum screen was used as a counter electrode.

Electrochemical measurements

Experiments were performed using a 50 mL three-electrode glass cell. The electrochemical testing procedure included measurements of OCP and EIS over a 48-hour period. OCP was measured during the 15 min before the EIS measurements. EIS was performed with OCP in a frequency range from 100 kHz to 10 mHz with 10 mV amplitude. PP was performed with a scan rate of 0.166 mV s^{-1} in a range potential of ± 25 mV from the cathodic to the anodic direction. All electrochemical experiments were performed at 23 ± 2°C in duplicate to ensure reproducibility. The electrochemical experiments were performed on a potentiostat/galvanostat Biologic VSP 300 with EC-Lab® software V10.32.

Sample preparation for electron microscopy

Ti6Al4V sections with adherent cells were rinsed with phosphate-buffered saline (PBS; 8.0 g of NaCl, 0.2 g of KCl, 1.4 g of $Na_2HPO_4{\cdot}2H_2O$ and 0.2 g L^{-1} of KH_2PO_4, pH = 7.2). The rinsed samples were fixed with glutaraldehyde 2.5% w/v in PBS for 2 h, followed by washing every 30 min. All fixation and washing steps were conducted at room temperature. After fixation, the cells were washed twice in PBS and then re-suspended in sterilised ultrapure water to avoid salt crystallisation during the drying process [17]. Finally, the samples were spattered with silver particles and observed by energy-dispersive spectroscopy under a JSM-7000F/JOEL microscope operated at 3–5 kV. Samples were also evaluated with high-resolution transmission electron microscopy and Field Emission Scanning Electron Microscopy using a SU5000 HITACHI variable pressure at high empty and 1 pascal.

Results and discussion

Impedance analysis documenting the growth of the biofilm on the alloy

The impact of bacteria and bacterial activity on the Ti6Al4V alloy was monitored by EIS. This technique is an ideal, non-destructive method that can be used to characterise processes carried out on electrode-dissolution interfaces. EIS provides the information needed to understand the process and to determine the nature of the underlying corrosion mechanism [34,35]. Impedance spectra are presented on a Nyquist plot as curves with different shapes that describe physicochemical phenomena within different frequency ranges (i.e. high, intermediate and low frequencies). At high frequencies ($f > 10^4$ Hz) the drop in ohms (iΩ) observed encompasses resistance to dissolution, conductor impedance and the geometry of the experimental apparatus. The maximum phase angle is displayed at intermediate frequencies (10^3–10 Hz) and the slope of the log Z *vs.* log *f* plot approaches −1. The capacitance (r) of the electrode is described in this region of frequencies, along with the dielectric properties of any film present on the electrode surface. At low frequencies ($f < 10$ Hz), the process of charge transfer (kinetics of the redox reaction), mass transfer (diffusion or ion migration) and/or other processes carried out on the interface or within the porosities of the metallic surface can be evaluated [36,37].

The results shown in Figure 1 represent the characteristic behaviour of Ti6Al4V (with surface passivation) under all conditions. In the absence of *E. coli,* evaluation of the Ti6Al4V electrodes revealed a typical corrosive process, including a decrease in charge transfer resistance (R_{ct}) observed in response to exposure to a saline medium. The opposite phenomenon was observed in the presence of *E. coli*. An increase in R_{ct} was observed beginning at 8 h and persisting until the end of the monitoring period. These data suggest that the adhesion and growth of *E. coli* on the Ti alloy were favoured under the conditions of this experiment and that bacteria that settled on the surface of the alloy interfered with the corrosion process.

The results included in the Nyquist plot shown in Figure 1 (a) did not include a clearly-defined semicircular loop. These findings indicated that the charge transfer was not favoured (i.e. that this was a slow process) because of significant capacitive effects together with other physical factors. The increase in R_{ct} observed between 8 and 32 h represents the initial formation of numerous active sites within the porosities of the passive layer of TiO_2 that facilitated specific adherence of *E. coli*. During their exponential growth phase, planktonic bacterial can spread to adhere over the entire surface of the alloy, thereby forming a barrier.

The results shown in the Bode plot (Figure 1(b)) represent the typical behaviour of the Ti6Al4V alloy under initial conditions (0 h). However, during the 24 h period that followed, we identified a second time constant corresponding to a coupled chemical process. This phenomenon can be attributed to the impact of *E. coli* metabolic processes, most notably the significant impact of redox reactions associated with glucose oxidation. After 32 h, this second constant disappeared, and the system returned to responses that were similar to those recorded under initial conditions over the next few hours. These findings may be the result of decreased bacterial activity due to nutrient depletion in the growth media and/or the formation of a biofilm over the surface of the Ti alloy [38].

As shown in Figure 2, two equivalent circuits were used to evaluate the formation of an *E. coli* biofilm. The impedance parameters of the alloy in the absence of bacteria were calculated as described in Figure 2(a). This method takes into account the physicochemical characteristics of this alloy and involves two-time constants because the passive layer of TiO_2 has a significant effect due to its high stability and porosity [39,40]. The model proposes that the oxide functions as a barrier-like inner layer while serving at the same time as a porous outer layer [41]. This same concept was used to illustrate the circuit (Figure 2(b)) and to calculate the impedance parameters for the biofilm. For this reason, a specific R_{ct} and constant phase element (CPE) were added to the circuit to account for the properties of the biofilm at its outermost part; this was based on the assumption that the *E. coli* was a significant factor and that 24 h will be sufficient time for the bacteria form a biofilm on the surface of Ti6Al4V under these conditions [26]. As noted in the Nyquist plot (Figure 1(a)) resistance increased over the first 8 h, suggesting that this assumption was valid. A biofilm is a well-organised community of microbial cells that display bacterially-derived chemical secretion products deposited at the extracellular matrix. These secreted biochemicals are mainly polysaccharides and proteins and include other substances [42] that influence the nature of the redox processes taking place at the surface of the alloy.

For the purposes of this study, the dielectric behaviour of the biofilm was considered to be a heterogeneous layer on the outer surface of the alloy. Therefore, the capacitive response of the interface was determined based on the properties of a non-ideal capacitor, i.e. one with a CPE used instead of a pure capacitance value which would be determined according to Equation (1) [43].

$$Z_{CPE} = \frac{1}{Y_0(j\omega)^n} \tag{1}$$

where

$$j = \sqrt{-1}\,;\ \omega = 2\pi f \tag{2}$$

CPE is an electrical element whose impedance is based on the angular frequency (ω), although the phase angle does not depend on time. Y_0 is a characteristic parameter and n ($-1 \leq n \leq 1$) is related to the rotation angle of a purely capacitive line [44]. It is critical to determine this value, as the CPE is related to the distribution of 'non-balance' current associated with surface roughness and other defects (e.g. porosity) and thus provides additional information on the physical properties of a biofilm. Therefore, in this model, we used a CPE to represent the actual capacitance instead of the ideal capacitance of the double layer [45]. The impact of the attraction or repulsion of electrical charges at the interface is described by n. The outer layer of a working electrode (passive layer with a metal coating, polymer, biofilm, or others) behaves like an ideal capacitor when $n = 1$ and the maximum phase angle is −90°. By contrast, $n = 0$ indicates this layer is functioning as a resistor and an inductor when $n = -1$ [46,47]. The CPE values were converted to double-layer capacitance (C_{dl}) using Equation (3), which is applicable for specific sections of the equivalent circuit because it relates to the R_{ct} of a

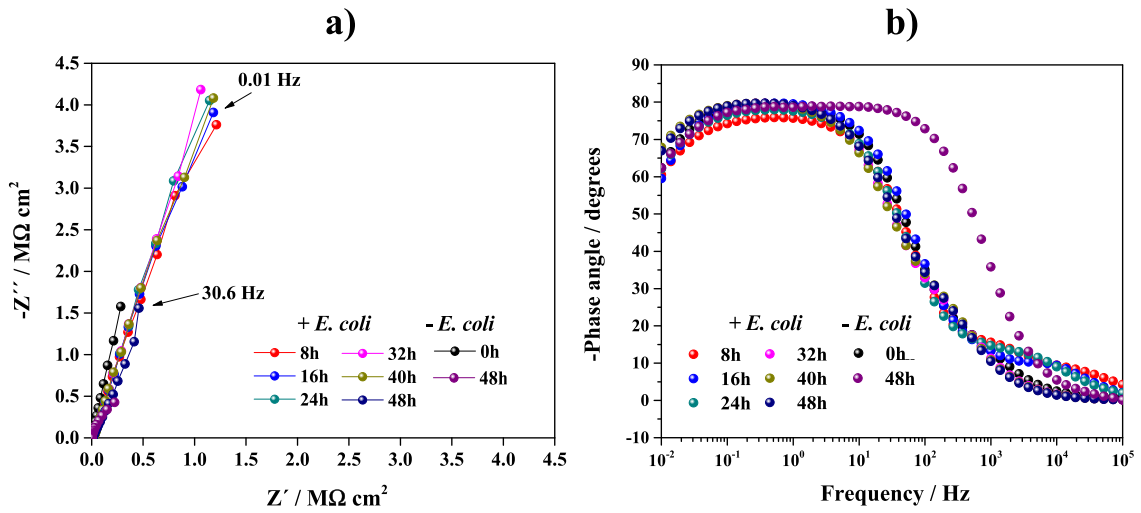

Figure 1. The behavior of Ti6Al4V alloy in the presence or absence of *E. coli* strain MC4100 in LB broth for 48 h; (a) Nyquist plot and (b) Bode plot.

particular time constant [48].

$$C_{dl} = \frac{(Y_0 R_{ct})^{\frac{1}{n}}}{R_{ct}} \sin\frac{n\pi}{2} \quad (3)$$

The impedance parameters obtained after monitoring for 48 h are shown in Table 2. In this instance, the biofilm behaved as a capacitor since the values of n (0.8–0.9) were close to 1 and maximum phase angles were between −75° and −80°, thus approximating the ideal value of −90°. The CPE values gradually increased up to a maximum of 5 s^n Ω^{-1} cm^{-2}; the same trend was observed for values of Rct_{-b}. The chi-square values (χ^2) were on the order of 10^{-3} and 10^{-4}, which indicated an excellent fit of the experimental data to the planned circuit using the CPE.

Impedance parameters (Rct_{-b} and C_{dl}) associated with the alloy in the presence of *E. coli* plotted against time showed a trend that was very similar to that displayed by standard graphs documenting exponential bacterial growth (i.e. number of bacteria *vs.* time) typically determined by UV-VIS spectroscopy [49]. The graphs of Rct_{-b} (Figure 3(a)) and C_{dl} (Figure 3(b)) revealed similar behaviour that also provided important information regarding bacterial growth and formation of the biofilm. During the first 16 h, the *E. coli* strain underwent adaptation at the surface of the alloy (i.e. the TiO_2 layer of Ti6Al4V) and the resistance observed increased slightly from 161.6 to 175.3 Ω cm^2; during this phase, the *E. coli* in the initial inoculum adapted to the environmental conditions and began to grow and divide and to adhere to the surface via the actions of cell wall proteins known as adhesins [8,50,51]. Subsequently (16–32 h) resistance increased due to the production of important bacterial exopolysaccharides; charge accumulated at the interface as a result of metabolic reactions and excretion of bacterial byproducts [52], which resulted in an increase in C_{dl} from 0.14 to 2.22 μF cm^{-2}. Biofilm then began to spread along the electrode surface. After 40 h, both the $R_{ct\text{-}b}$ and the C_{dl} remained constant. These latter results suggested that the bacteria had entered the stationary phase and that the biofilm on the surface of the alloy had matured. Similar results were reported by Zheng et al. [53] in a study that was carried out with sulfate-reducing bacteria; similar to our results, this group reported an increase in R_{ct} at the beginning of the monitoring period followed by a progressive decline at the end of the experiment. Similar behaviour was reported by Calvillo and Galicia [16], who presented impedance diagrams that illustrate times for adherence and attachment of *Shewanella sp.* in a marine biofilm. Our findings were also analogous to those of Castaneda and Galicia [17] who identified an extra biolayer originating from a sulfate-reducing bacterial consortium based on the synthesis and release of EPS that influenced the homogeneous biolayer.

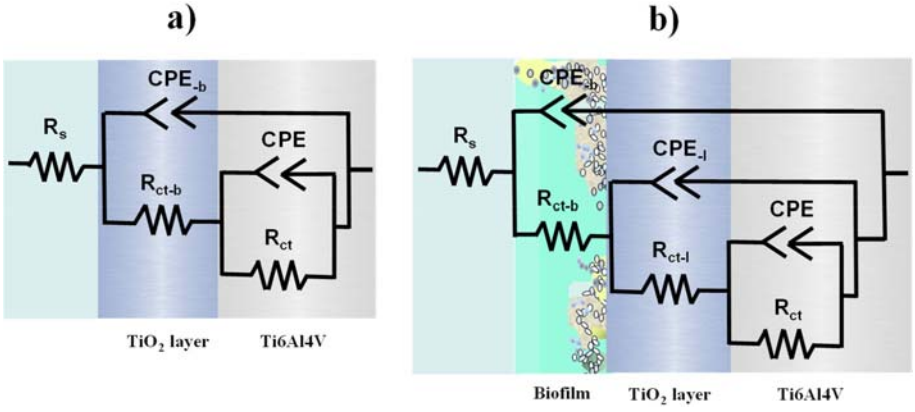

Figure 2. Equivalent circuits used for the calculation of impedance parameters; (a) circuit for Ti6Al4V in the absence of *E. coli* (control) and (b) circuit for Ti6Al4V together with *E. coli*.

Table 2. Parameters documenting the fit from an equivalent circuit simulation for Ti6Al4V alone and in the presence of *E. coli* over varying times.

Time (h)	R_s (Ω cm^2)	CPE_{-b} ($s^n\ \Omega^{-1}$ cm^{-2})	n_{-b}	C_{dl} (μF cm^{-2})	$R_{ct\text{-}b}$ (Ω cm^2)	CPE_{-l} ($s^n\ \Omega^{-1}$ cm^{-2})	$R_{ct\text{-}l}$ (Ω cm^2)	CPE ($s^n\ \Omega^{-1}$ cm^{-2})	R_{ct} (MΩ cm^2)	χ^2
Ti6Al4V with *E. coli*										
8	364.7	0.35×10^{-6}	0.8	0.03	161.6	2.76×10^{-6}	406.3	4.18×10^{-6}	4.46	6.4×10^{-4}
16	368.4	0.42×10^{-6}	0.9	0.14	175.3	2.67×10^{-6}	359.4	3.10×10^{-6}	4.59	3.7×10^{-3}
24	375.6	1.63×10^{-6}	0.8	0.24	290.9	2.79×10^{-6}	371.4	3.35×10^{-6}	4.56	4.2×10^{-3}
32	377.9	4.33×10^{-6}	0.9	2.22	566.4	2.41×10^{-6}	380.6	3.59×10^{-6}	4.56	9.7×10^{-4}
40	369.5	4.77×10^{-6}	0.9	2.53	714.6	2.67×10^{-6}	400.9	3.31×10^{-6}	4.60	7.5×10^{-3}
48	378.8	4.84×10^{-6}	0.9	2.58	728.1	2.64×10^{-6}	386.8	2.41×10^{-6}	4.63	4.8×10^{-4}
Ti6Al4V without *E. coli*										
0	354.9	–	–	–	–	1.94	375.4	2.84	4.2	8.1×10^{-3}
48	363.4	–	–	–	–	21.6	416.5	5.54	1.9	1.2×10^{-4}

Note: $R_{ct\text{-}b}$ is charge transfer resistance of biofilm, $R_{ct\text{-}l}$ is charge transfer resistance for TiO_2 layer in presence of biolfilm.

PP analysis

Tafel curves for Ti6Al4V in the absence and presence of bacteria during a 48 h monitoring period are shown in Figure 4, and the associated corrosion parameters are presented in Table 3. Ti6Al4V in the absence of *E. coli* generated a typical polarisation curve with a well-defined passivation zone (i.e. a passive plateau region) between 0.5 and 1.2 V *versus* a saturated calomel electrode (SCE). The effect of the biofilm (line B) was evident because the passive plateau was distorted over the same range of potentials. This finding may be due to the formation of a more heterogeneous passive layer that favoured the formation of a biofilm along its surface.

The corrosion rate (C_r) was 1.42×10^{-4} mm year^{-1} in the absence of *E. coli*. The presence of bacteria resulted in a significant decrease in C_r. This finding confirmed the impedance analyses and the concept that the biofilm may be serving as a protective barrier. This could be attributed to the favourable conditions promoting bacterial growth within the pores of the TiO_2 layer. Bacterial growth and biofilm formation may ultimately prevent the flow of oxidising agents to the alloy, potentially due to the actions of biomolecules, including lipopolysaccharides (LPS), as well as proteins, and other components of the Gram-negative bacteria outer membrane [54]. These results are consistent with findings reported previously by other investigations who also found that the *E. coli* biofilm acts as a protective layer during the growth phase (0–40 h) [27]. This interpretation is also supported by the findings presented in Figure 3(a) that document the relationship between Rct_{-b} and time over a longer period.

Figure 5 includes a diagram of an *E. coli* biofilm formed on the surface of Ti6Al4V that includes the most important

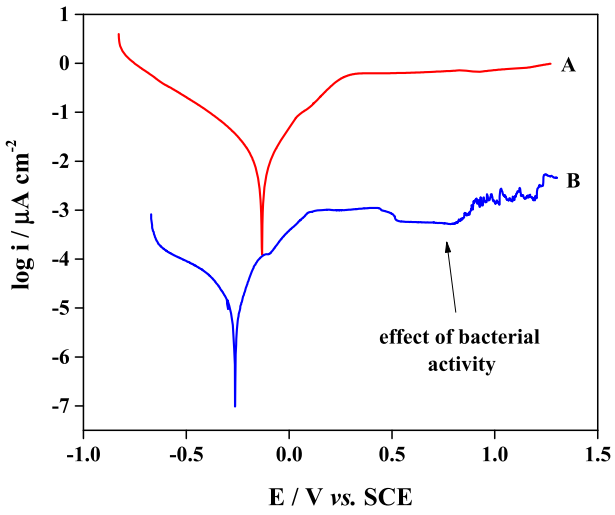

Figure 4. Tafel plot documenting responses at 48 h to (A) Ti6Al4V in the absence of *E. coli* and (B) Ti6Al4V in the presence of *E. coli*.

chemical and electrochemical processes. Under aerobic conditions, the biofilm establishes itself in the outer passive layer of the alloy. Once the bacteria have settled, *E. coli* generates metabolic byproducts that contribute to the corrosion process, including the production of CO_2 from the oxidation of glucose. In an aqueous medium, this results in the accumulation of H_2CO_3 that ultimately dissociates, thereby releasing H^+ ions. This mechanism was introduced by Banaszek et al. [55] who explained that *E. coli* could influence corrosion and the deterioration of metal surfaces via the production and release of corrosive microbial byproducts. However, the surface of the Ti did not undergo deterioration

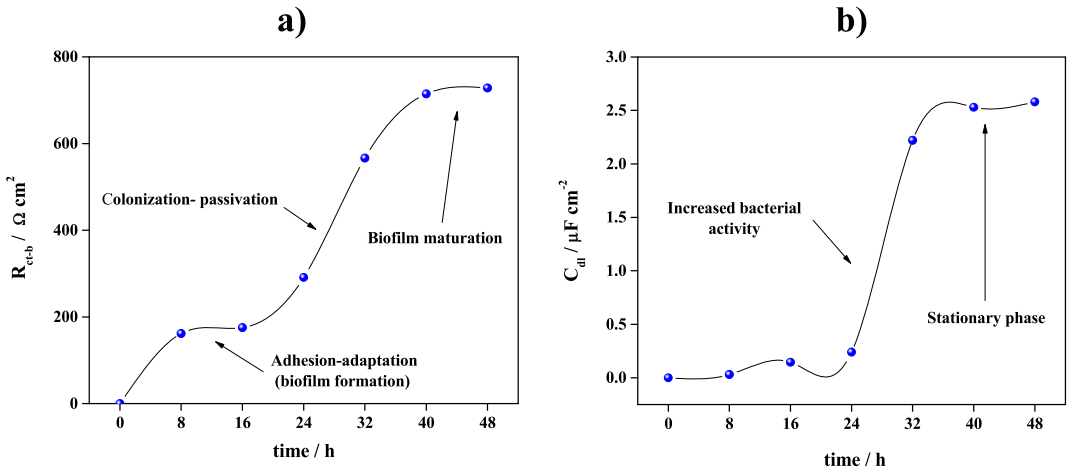

Figure 3. Diagram of biofilm formation based on measured impedance parameters, including (a) $R_{ct\text{-}b}$ *vs.* time and (b) C_{dl} *vs.* time.

Table 3. PP information about the corrosion process of Ti6Al4V on different conditions.

Ti6Al4V with *E. coli* (48h)	−266.4	0.042 (0.001)	259.2	345.2	3.55×10^{-6} (1.13×10^{-7})
Ti6Al4V without *E. coli* (48h)	−132.2	9.1 (0.14)	176.5	212.2	1.42×10^{-4} (2.55×10^{-6})
Electrode	E_{corr} (mV)	i_{corr} (nA cm^{-2})	β_a (mV/dec)	β_c (mV/dec)	C_r (mm year)

Note: Standard deviation (SD) indicated within the parentheses, $n = 3$.

because the kinetics in the acidic medium favoured the formation of corrosion products (i.e. Ti_xO_y) that gave rise to the passive layer of TiO_2 via the relationships described below:

$$2Ti + 3H_2O \rightarrow Ti_2O_3 + 6H^+ + 6e \quad (4)$$

$$Ti_2O_3 + 3H_2O \rightarrow 2TiO(OH)_2 + 2H^+ + 2e^- \quad (5)$$

$$Ti + 3H_2O \rightarrow TiO(OH)_2 + 4H^+ + 4e^- \quad (6)$$

A final dehydration step leads to the formation of TiO_2:

$$TiO(OH)_2 \rightarrow TiO_2 + H_2O \quad (7)$$

The global reaction is described by Equation 8.

$$Ti + 2H_2O \rightarrow TiO_2 + 4H^+ + 4e^- \quad (8)$$

These reactions are highly favoured and occur nearly instantly, as the oxygen reduction reaction serves to complement the redox reaction. This process is also favoured in the presence of catalysts that promote the reduction of oxygen [56]. Given this relationship, the bacteria do not corrode the alloy but instead contribute to the formation of a more stable, rigid and amorphous passive layer [57]. This in turn favours the formation of connections between bacterial cells within the surface porosities, thereby promoting the growth of the biofilm.

Characterisation of the E. coli *biofilm by SEM*

Figure 6 includes a top-view SEM image of the Ti6Al4V alloy before it was immersed into the bio-electrolyte medium. Microstructural analyses were performed at a magnification of 1000×.

We assessed the initial structural characteristics of the Ti6Al4V alloy and detected micropores and micro-rays on the two working electrodes that were generated by manual

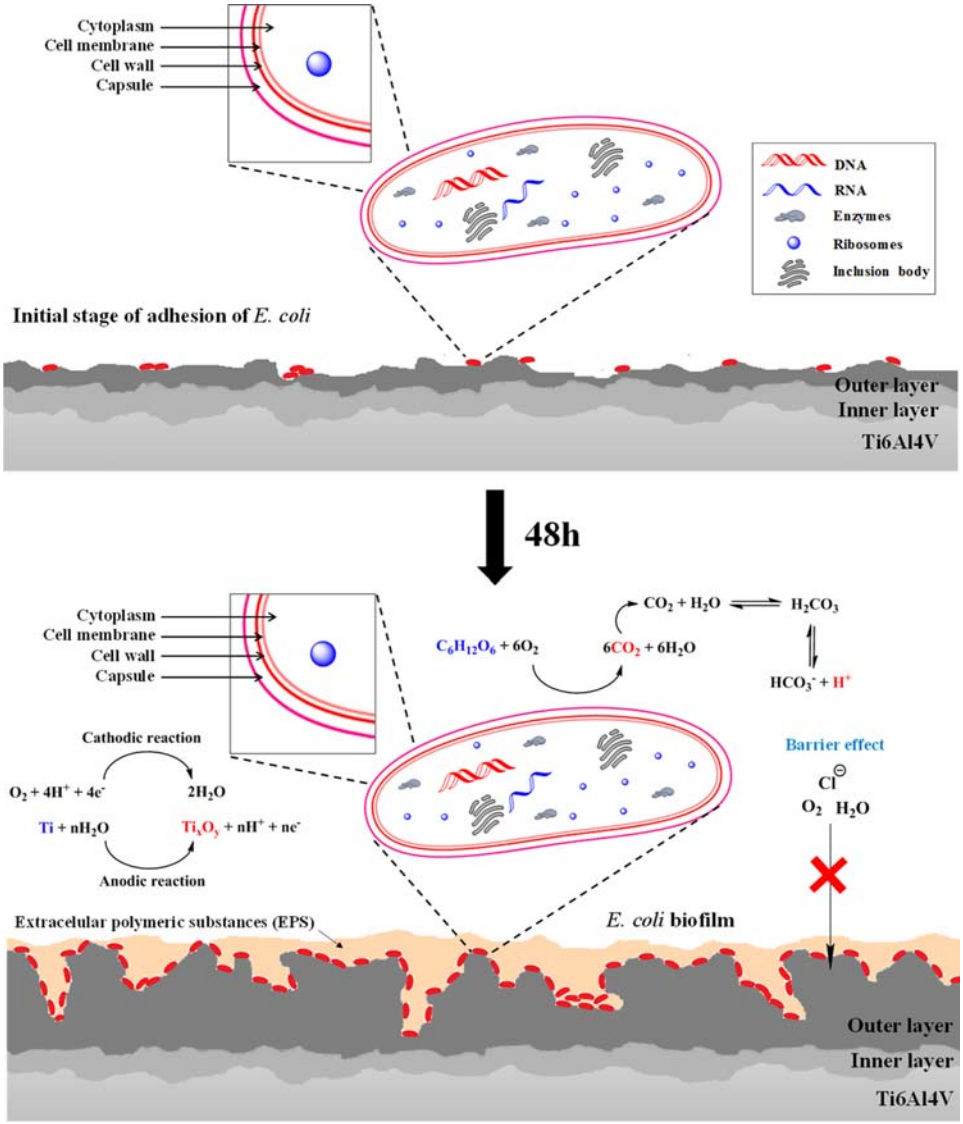

Figure 5. Schematic outlining the process of formation of *E. coli* biofilms on Ti6Al4V.

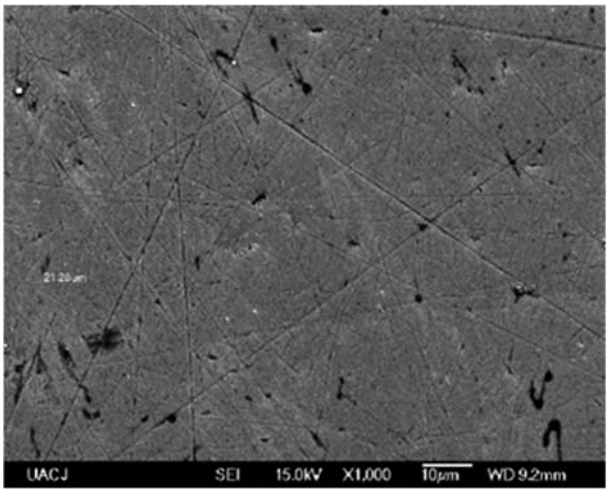

Figure 6. Top-view SEM image of the Ti6Al4V alloy before its immersion in a bio-electrolyte medium; original magnification, 1000×.

polishing (mirror termination). We verified the absence of any type of corrosion before initiating the experiment. SEM images of the Ti6Al4V taken after exposure to *E. coli* in the bacterial culture medium are shown in Figure 7(a,b). Magnifications of 6500× and 10 000× were used to resolve individual bacteria that are typically between 2 and 5 μm in length. As shown in Figure 7(a), several colonies of bacteria are visualised as single bacilli. This finding suggests that each of these clusters was formed by a single bacilli cells that replicated to form a colony. Similarly, the results suggest that optimal growth conditions for bacterial colonies had been established, as the culture medium (LB agar) adhered perfectly to the surface of the alloy. The *E. coli* biofilm that developed in LB medium was detected as small, distinct cells.

The image in Figure 7(b) documents the sizes of the individual bacterial cells ranging from 0.700 μm to nearly 2 μm in length. This image also confirms the presence of bacterial colonies on the surface of the Ti6Al4V alloy. The adherence factors promoting colonisation might include the culture medium, the porosity of the alloy surface and the size and shape of the bacterial cells. The biofilm consisted primarily of a layer of sessile cells near the biofilm-metal interface; a larger number of live cells are typically present at higher temperatures [58–60].

The morphologies of the *E. coli* colonies shown in Figure 7b include both the rough and smooth forms. Rough colonies can be described as coarse, flat and irregular, whereas smooth colonies are more regular, high and circular in shape. Collectively, the colony morphologies identified in Figure 7(a–c) correspond to colonies of *E. coli*. Also, Figure 7 (c) provides more precise evidence for the formation of a biofilm as indicated by the presence of a thin layer of EPS associated with *E.coli* bacterial aggregates. Biofilm formation associated with the presence of bacteria colonies has been reported in previous investigations featuring different media [15].

The micropores detected in this alloy sample were somewhat smaller than anticipated because a passive layer was generated on the working electrode. Corrosion of metal alloys can be inhibited by a homogenous biofilm at a certain minimum biofilm thickness or density. The absence of a polysaccharide matrix can result in the detachment of the cells as shown in Figure 7(a,b). Under these conditions, oxygen will be able to react with the metal surface and promote

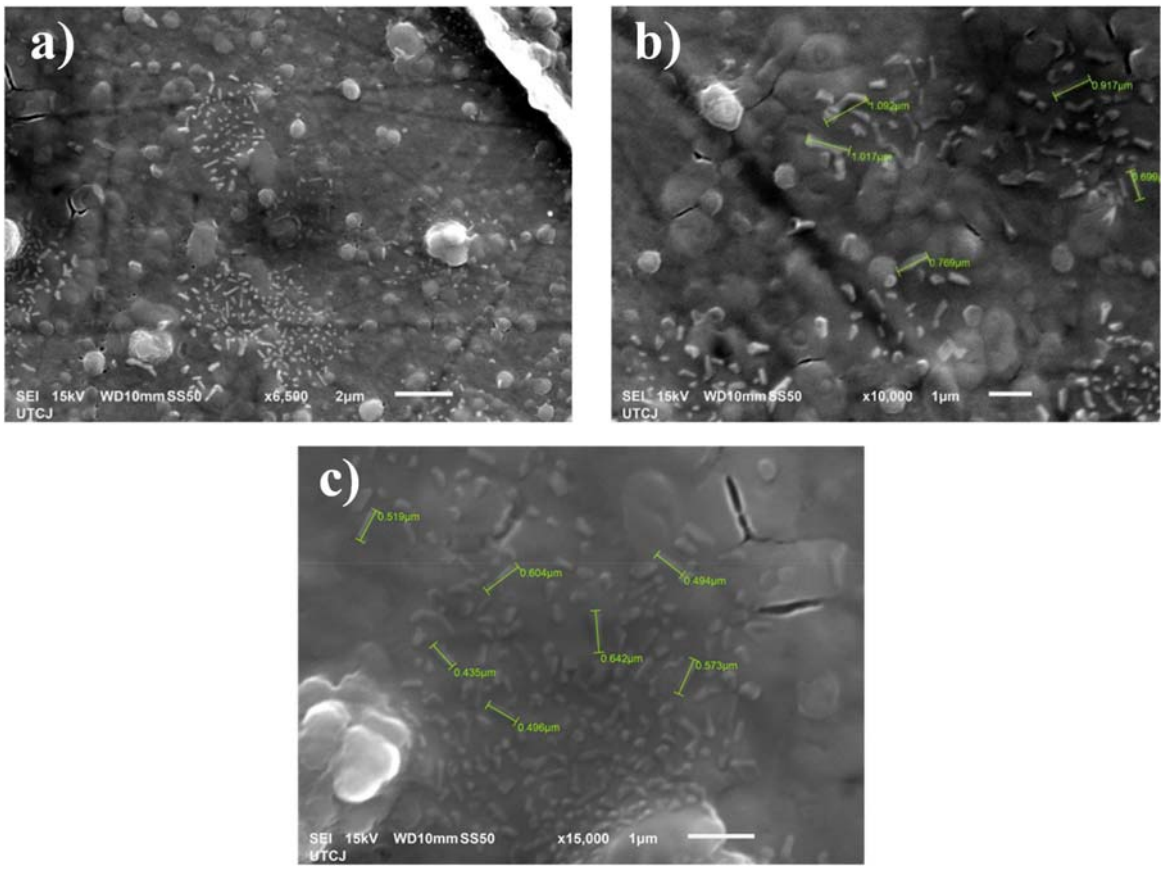

Figure 7. Top-view SEM images of *E. coli* biofilms on the Ti6Al4V alloy after 48 h of exposure; original magnifications (a) 6500×, (b) 10 000× and (c) 15 000×.

corrosion. However, the formation of an initial thin layer of biofilm as shown in Figure 7(c) and confirmed with electrochemical results as shown by the Tafel plots (Figure 4) resulted in a decrease in corrosion rate in presence of a bio-electrolyte solution. This finding may be attributed to the fact that a uniform distribution was achieved only after 48 h of exposure. Development of the thin, homogeneous layer may serve to reduce the amount of dissolved oxygen available to promote corrosion at some sites within the metal surface [15,56,57]. This interpretation is consistent with the findings from impedance analysis, which suggested that the corrosion *versus* inhibition processes predominated at different stages of bacterial growth. Rct_{-1} increased between 16 and 32 h during the time required for biofilm formation. Charge transfer resistance decreased from 24 to 40 h, which suggests detachment of the biofilm and an increase in the rate of corrosion. Similar findings were reported in previous studies that focused on the assessment of corrosion of coatings in an electrolyte solution with a bacterial consortium [17]. However, a slight stabilisation of the impedance parameter was detected at 48 h, which may denote the formation of a new biofilm at the metallic surface.

Conclusions

Impedance parameters associated with the formation of biofilms, $R_{ct\text{-}b}$ and C_{dl}, presented with trends that were similar to those reported in graphs of bacterial growth over time, i.e. exponential growth as detected by UV-VIS spectroscopy. *E. coli* in growth medium suspension forms a biofilm on the surface of Ti6Al4V that can be detected after 48 h of exposure. The behaviour of this biofilm was described using analogue circuit parameters. The initial impact of electrochemical factors and the formation of the bacterial biofilm can result in either corrosion or its inhibition. A new uniform biofilm appears to form between 40 and 48 h. SEM images document the production of EPS during this interval in association with biofilm formation and its subsequent detachment. This process was associated with a significant drop in pH, which may have resulted from the growth and proliferation of these bacteria. Increases in resistance (R_{ct}) that develop between 8 and 32 h indicated the initial formation of numerous active sites at which *E. coli* specifically adhered to porosities within the passive layer of TiO_2. However, with time and in accordance with the variables described, including depletion of critical nutrients and detachment of the EPS, the biofilm was unable to undergo consolidation. Therefore, the mechanisms presented to explain biofilm formation and its capacity to inhibit corrosion inhibition are not only plausible, they also serve to predict the behaviour of other microorganisms in the marine environment upon exposure to an alloy surface under aerobic conditions for a brief period of time.

Acknowledgements

This work was supported by Laboratorio de Microscopía e Investigación Matemática of Universidad Tecnológica de Ciudad Juárez. The authors acknowledge the technical support provided by Hortensia Reyes Blas, Ruth Saraí Romero Domínguez, Jacobo Recio Hernández, and the use of microbiological infrastructure of Laboratorio de Biología Celular y Molecular at UACJ.

Disclosure statement

No potential conflict of interest was reported by the author(s).

ORCID

Jonathan Calvillo http://orcid.org/0000-0003-2928-488X
Mónica Galicia http://orcid.org/0000-0003-1273-3204
Roxana Malpica http://orcid.org/0000-0002-4933-3071
Elsa Ordoñez http://orcid.org/0000-0002-8970-5730
Héctor Ferral Pérez http://orcid.org/0000-0002-1706-3281

References

[1] Alaeddine K, Khedidja B. Electrochemical boriding of titanium alloy Ti-6Al-4V. J Mater Res Technol. 2019;8(6):6407–6412.
[2] Lin N, Huang X, Zhang X, et al. In vitro assessments on bacterial adhesion and corrosion performance of TiN coating on Ti6Al4V titanium alloy synthesized by multi-arc ion plating. Appl Surf Sci 2012;258(18):7047–7051.
[3] Güleryüz H, Cimenoglu H. Effect of thermal oxidation on corrosion and corrosion–wear behaviour of a Ti–6Al–4V alloy. Biomaterials. 2004;25(16):3325–3333.
[4] Toptan F, Alves AC, Carvalho O, et al. Corrosion and tribocorrosion behaviour of Ti6Al4V produced by selective laser melting and hot pressing in comparison with the commercial alloy. J Mater Process Technol 2019;266(1):239–245.
[5] Ren L, Ma Z, Li M, et al. Antibacterial properties of Ti–6Al–4V–xCu alloys. J Mater Sci Technol 2014;30(7):699–705.
[6] Prasad K, Bazaka O, Chua M, et al. Metallic biomaterials: current challenges and opportunities. Materials (Basel). 2017;10(8):884–918.
[7] Manivasagam G, Dhinasekaran D, Rajamanickam A. Biomedical implants: corrosion and its prevention – A review~!2009-12-22~!2010-01-20~!2010-05-25~!. Recent Pat Corros Sci. 2010;2(2):40–54.
[8] Kip N, van Veen J. The dual role of microbes in corrosion. ISME J. 2015;9(1):542–551.
[9] Sharan J, Lale SV, Koul V, et al. An overview of surface modifications of titanium and its alloys for biomedical applications. Trends Biomater Artif Organs. 2015;29(2):176–187.
[10] Liu R, Tang Y, Zeng L, et al. *In vitro* and *in vivo* studies of antibacterial copper-bearing titanium alloy for dental application. Dent Mater 2018;34(8):1112–1126.
[11] Guan F, Zhai X, Duan J, et al. Influence of sulfate-reducing bacteria on the corrosion behavior of high strength steel EQ70 under cathodic polarization. PloS one. 2016;11(9):1–22.
[12] Eliaz N. Corrosion of metallic biomaterials: a review. Materials. 2019;12(3):407–499.
[13] Fariña J, Rehm B, Sieber V, et al. Editorial: Microbial Exopolysaccharides: From Genes to Applications. Front Microbiol 2016;7(1):1–308.
[14] Fleeming HC, Wingende J. The biofilm matrix. Nat Rev Microbiol. 2010;8:623–633.
[15] Galicia M, Valencia Goujon V, Aguirre-Ramírez M, Castaneda H. NACE - International Corrosion Conference Series, 2017, 6, pp. 3786–3799.
[16] Calvillo Solís JJ, Galicia García M. Electrochemical Behavior of Zn-REP Nano-hybrid Coatings during Marine Shewanella sp. Biofilm Formation. Mater Corros. 2021, 1–15. doi:10.1002/maco.202011997.
[17] Castaneda H, Galicia M. Corrosion Assessment of Zn-Rich Epoxy Primers With Carbon Nanotube Additions in an Electrolyte With a Bacteria Consortium. Front Mater. 2019;6(307):1–12.
[18] Gode C, Attarilar S, Eghbali B, et al. Electrochemical behavior of equal channel angular pressed titanium for biomedical application. AIP Conf Proc 2015;1653(020041):1–10.
[19] Attarilar S, Djavanroodi F, Irfan OM, et al. Strain uniformity footprint on mechanical performance and erosion-corrosion behavior of equal channel angular pressed pure titanium. Results Phys 2020;17(103141):1–9.

[20] Xue T, Attarilar S, Liu S, et al. Surface Modification Techniques of Titanium and its Alloys to Functionally Optimize Their Biomedical Properties: Thematic Review. Front Bioeng Biotechnol 2020;8(603072):1–19.
[21] Dhaliwal JS, Rahman N, Knights J, et al. The effect of different surface topographies of titanium implants on bacterial biofilm: a systematic review. SN Appl Sci. 2019;1(6):1–16.
[22] Attarilar S, Yang J, Ebrahimi M, et al. The Toxicity Phenomenon and the Related Occurrence in Metal and Metal Oxide Nanoparticles: A Brief Review From the Biomedical Perspective. Front Bioeng Biotechnol. 2020;8(822):1–23.
[23] Liu J, Liu J, Attarilar S, et al. Nano-Modified Titanium Implant Materials: A Way Toward Improved Antibacterial Properties. Front Bioeng Biotechnol. 2020;8(576969):1–30.
[24] Wang Q, Zhou P, Liu S, et al. Multi-Scale Surface Treatments of Titanium Implants for Rapid Osseointegration: A Review. Nanomaterials. 2020;10(1244):1–27.
[25] Cwalina B, Dec W, Michalska J, et al. Initial stage of the biofilm formation on the niTi and Ti6Al4V surface by the sulphur-oxidizing bacteria and sulphate-reducing bacteria. J Mater Sci: Mater Med 2017;28(11):173–184.
[26] Ma Z, Bumunang EW, Kim Stanford K, et al. Biofilm formation by shiga toxin-producing *Escherichia coli* on stainless steel coupons as affected by temperature and incubation time. Microorganisms. 2019;7(4):95.
[27] Dong J, Fang D, Zhang L, et al. Gallium-doped titania nanotubes elicit anti-bacterial efficacy *in vivo* against *Escherichia coli* and staphylococcus aureus biofilm. Materialia. 2019;5:100209.
[28] Malhotra R, Dhawan B, Garg B, et al. A comparison of bacterial adhesion and biofilm formation on commonly used orthopaedic metal implant materials: an *in vitro* study. Indian J Orthop. 2019;53(1):148–153.
[29] Shick-Yu T. Effect of titanium-ion on the growth of various bacterial species. J Microbiol 2004;42(1):47–56.
[30] Barão V, Mathew M, Assunção W, et al. The role of lipopolysaccharide on the electrochemical behavior of titanium. J Dent Res 2011;90(90):613–618.
[31] Chaturvedi T. An overview of the corrosion aspect of dental implants (titanium and its alloys). Indian J Dent Res. 2009;20 (1):91–98.
[32] Walkowiak M, Klimek L, Okrój W, et al. Adhesion, activation, and aggregation of blood platelets and biofilm formation on the surfaces of titanium alloys Ti6Al4V and Ti6Al7Nb. J Biomed Mater Res Part A. 2012;100A(3):768–775.
[33] Cortez V, Oliveira A, Aguilar C, et al. Corrosion behavior analysis of plasma-assited PVD coated Ti-6Al-4V alloy in 2 M NaOH solution. Mater Res. 2017;20(2):436–444.
[34] Zhou T, Liu J, Zhang X, et al. The antibacterial W-containing microarc oxidation coating on Ti6Al4V. Surf Coat Technol 2019;374(1):242–252.
[35] Khan M, Williams R, Williams D. The corrosion behaviour of Ti–6Al–4V, Ti–6Al–7Nb and Ti–13Nb–13Zr in protein solutions. Biomaterials. 1999;20(7):631–637.
[36] Ghoneim A, Mogoda A, Awad A, et al. Electrochemical studies of titanium and its Ti–6Al–4V alloy in phosphoric acid solutions. Int J Electrochem Sci 2012;7(1):6539–6554.
[37] Motalebi A, Nasr-Esfahani M. Electrochemical and In vitro behavior of nanostructure Sol-Gel coated 316L stainless steel incorporated with rosemary extract. J Mater Eng Perform 2013;22(1):1756–1764.
[38] Advincula C, Petersen D, Rahemtulla F, et al. Surface analysis and biocorrosion properties of nanostructured surface sol–gel coatings on Ti6Al4V titanium alloy implants. J Biomed Mater Res B Appl Biomater 2007;80B(1):107–120.
[39] Metikos M, Kwokal A, Piljac J. The influence of niobium and vanadium on passivity of titanium-based implants in physiological solution. Biomaterials. 2003;24(21):3765–3775.
[40] Souza J, Ponthiaux P, Henriques M, et al. Corrosion behaviour of titanium in the presence of streptococcus mutans. J Dent 2013;41 (6):528–534.
[41] Pacha M, Gallardo A, Vadillo V, et al. Electrochemical analysis of the UV treated bactericidal Ti6Al4V surfaces. Mater Sci Eng C. 2013;33(3):1789–1794.
[42] de Assis S, Wolynec S, Costa I. Corrosion characterization of titanium alloys by electrochemical techniques. Electrochim Acta. 2006;51(8-9):1815–1819.
[43] Alves V, Reis R, Santos L, et al. In situ impedance spectroscopy study of the electrochemical corrosion of Ti and Ti–6Al–4V in simulated body fluid at 25°C and 37°C. Corros Sci 2009;51 (10):2473–2482.
[44] Mathew M, Barão V, Yuan J, et al. What is the role of lipopolysaccharide on the tribocorrosive behavior of titanium?. J Mech Behav Biomed Mater 2012;8(1):71–85.
[45] Wen R, Yang C, Huang C, et al. Investigation on the corrosion behavior of Ti–6Al–4V implant alloy by electrochemical techniques. Mater Chem Phys 2004;86(2-3):269–278.
[46] Barranco V, Escudero M, García M. 3D, chemical and electrochemical characterization of blasted TI6Al4V surfaces: Its influence on the corrosion behaviour. Electrochim Acta. 2007;52(2):4374–4384.
[47] Gallardo J, Durán A, de Damborenea J. Electrochemical and *in vitro* behaviour of sol–gel coated 316L stainless steel. Corros Sci 2004;46(4):795–806.
[48] Chang BY. Conversion of a constant phase element to an equivalent capacitor. J Electrochem Sci Technol. 2020;11 (3):318–321.
[49] Kacena M, Merrell G, Manfredi B, et al. Bacterial growth in space flight: logistic growth curve parameters for *Escherichia coli* and bacillus subtilis. Appl Microbiol Biotechnol 1999;51(2):229–234.
[50] Fonseca C, Barbosa M. Corrosion behaviour of titanium in biofluids containing H2O2 studied by electrochemical impedance spectroscopy. Corros Sci. 2001;43(3):547–559.
[51] Faverani L, Assunção W, de Carvalho P, et al. Effects of dextrose and lipopolysaccharide on the corrosion behavior of a Ti-6Al-4V alloy with a smooth surface or treated with double-acid-etching. Plos one. 2014;9(3):1–15.
[52] Dexter S. Role of microfouling organisms in marine corrosion†. Biofouling. 1993;7(1):97–127.
[53] Zheng X, Zhuang X, Lei Y, et al. Corrosion behavior of the Ti–6Al–4V alloy in sulfate-reducing bacteria solution. Coatings. 2020;10(1):24–36.
[54] Guo S, Lu Y, Wu S, et al. Preliminary study on the corrosion resistance, antibacterial activity and cytotoxicity of selective-laser-melted Ti6Al4V- x Cu alloys. Mater Sci Eng C. 2017;72 (1):631–640.
[55] Banaszek K, Szymanski W, Pietrzyk B, et al. Adhesion of *E. coli* bacteria cells to prosthodontic alloys surfaces modified by TiO_2 Sol-Gel coatings. Adv Mater Sci Eng. 2013;1(1):1–6.
[56] Pope D, Duquette D, Wayner P. Mater Performance. 1984;14 (1):14–18.
[57] Schneider B, Sopchenski L, de Araújo H, et al. Electrochemical stability and bioactivity evaluation of Ti6Al4V surface coated with thin oxide by EIS for biomedical applications. Mater Res. 2015;18(3):602–607.
[58] Shah F, Trobos M, Thomsen P, et al. Commercially pure titanium (cp-Ti) versus titanium alloy (Ti6Al4V) materials as bone anchored implants – Is one truly better than the other?. Mat Sci Eng C. 2016;62(2):960–966.
[59] Rodrigues D, Valderrama P, Wilson T, et al. Titanium corrosion mechanisms in the oral environment: a retrieval study. Materials. 2013;6(11):5258–5274.
[60] Lorenzetti M, Dogsa I, Stosicki T, et al. The influence of surface modification on bacterial adhesion to titanium-based substrates. Appl Mater Interf. 2015;7(3):1644–1651.